A Parallel Connected Hybrid Microstrip-Substrate Integrated Waveguide Bandstop Filter

Kemal Guvenli[1,*], Sibel Yenikaya[2], Mustafa Secmen[3]
[1]Department of Electronics and Automation, Hitit University, North Campus, 19100, Corum, Turkey
[2]Department of Electrical and Electronics Engineering, Bursa Uludag University, Gorukle Campus, 16100, Nilufer, Bursa, Turkey
[3]Department of Electrical and Electronics Engineering, Yasar University, University Street, Nos: 37–39, 35100, Bornova, Izmir, Turkey
[*]kemalguvenli@hitit.edu.tr; sguler@uludag.edu.tr; mustafa.secmen@yasar.edu.tr

***Abstract*—This study presents an original parallel connected hybrid microstrip-substrate integrated waveguide (PCHM-SIW) bandstop filter. A low-pass filter implemented on a microstrip structure and a SIW-based high-pass filter are connected in parallel to each other. In this way, the aim is to obtain a bandstop filter in the novel hybrid design. The parallel connected hybrid microstrip-substrate integrated waveguide (PCHM-SIW) bandstop filter is synthesised, simulated, and produced. The effects of connecting filters in parallel are discussed. It is seen from the results of CST Studio Suite simulation that PCHM-SIW bandstop filter has a bandwidth of 2.85 GHz and a center frequency of 4.26 GHz. The frequency change rate of the center frequency between simulation and measurement is 7.02 % where it is just 3.76 % for the deviation in bandwidth. The results of the simulation and those of the measurement are close to each other. These results converge to ideal analytical results.**

***Index Terms*—Substrate integrated waveguide; Microstrip; Parallel integration; X-band; Hybrid bandstop filter.**

I. INTRODUCTION

As is known, filters are devices that allow some signals to pass whereas the rest do not. Especially in wireless communication technology (cellular systems), microwave filters are one of the basic circuit structures. Highly efficient microwave filters are required to minimise interference and use the frequency spectrum at full capacity in cellular systems [1].

After the 90s, the trend of personal communication started to rise. Fifth generation devices (5G) with 1 Gbps speed have been actively used in mobile base stations in wireless communication. Due to the increasing data and efficiency demand in these devices, the importance of microwave filters has increased even more.

In the literature, various techniques such as substrate integrated waveguide (SIW) microstrip structure [2], dielectric resonator [3], liquid crystal (LC) material [4], defective ground plane (DGS) [5], coaxial resonator [6], RF MEMS switches [7], and open-circuited shunt stub [8] are applied to produce a band stop filter. The focus has been on the SIW architecture because of its easy integration, low cost, expandability, and efficient high-frequency characteristics. Therefore, microstrip and SIW structures are used in the design of the parallel connected hybrid microstrip-substrate integrated waveguide (PCHM-SIW) bandstop filter.

The design of the PCHM-SIW bandstop filter is presented in three steps. A high-pass filter and a low-pass filter are modelled in the first and second steps, respectively. The PCHM-SIW bandstop filter is obtained by connecting two structures in the first and second phases in parallel. The approach to designing a parallel connected bandstop filter is to create a bandstop filter from the sum of the frequency responses of the low- and high-pass filters. A bandstop filter effect is generated by the intersection of nonpassing regions of low-pass and high-pass filters. In this way, a bandstop frequency region is obtained. If these filter structures are connected in series, it becomes an all-stop filter, which does not allow to pass any frequency. Although it may seem complicated to connect SIW and microstrip-based structures in parallel to obtain a stopband filter, this simple design is preferred due to the clarity of determining the stopband and passband frequency regions. In this way, the bandstop filter design can be easily revised for different desired frequency regions. This method helps to flexibly design a bandstop filter.

In this study, the proposed structure is verified by combining a Chebyshev microstrip-based low-pass filter and a SIW-based high-pass filter. The length of each section of the fifth-order Chebyshev microstrip low-pass filter parameter is selected as $\lambda_{lpf}/8$ where λ_{lpf} is the effective wavelength of the microstrip transmission line above the substrate. The connection between the microstrip-based structure and the SIW-based structure is like a conical section [9]. There is an angle of 120 ° between the low-pass filter microstrip line and the high-pass filter microstrip line to shorten the transmission line. The frequency response of the SIW-based structure, which is a planar rectangular waveguide that we can call a two-dimensional structure, is preferred at high frequencies compared to other filter structures, since it has high return loss in addition to low insertion loss in pass band. Therefore, the SIW-based

Manuscript received 27 June, 2023; accepted 21 October, 2023.

structure is chosen due to its low-loss and thermal stability [2], [6], [10]. Moreover, unlike previous studies, an original hybrid bandstop filter structure was designed by combining one low-pass filter and one high-pass filter structure being parallel to each other.

II. THE PARALLEL CONNECTED HYBRID FILTER DESIGN

The bandstop filter design consists of a low-pass filter based on short-length microstrip lines and a SIW-based high-pass filter. These two structures are parallel to each other. The bandstop filter is designed to suppress signals between 3.75 GHz and 6.60 GHz, including the S-Band and C-Band. The low-pass filter passes signals in the 0 GHz–3.75 GHz range. The high-pass filter passes signals above 6.6 GHz. This might be called the frequency switching method (FSM). In the design, the parallel connection angle between the two filters is determined as 120 degrees. Consequently, the designed filter exhibits a bandstop filter behaviour. According to the analysis, the stopband frequency range is 3.75 GHz–6.6 GHz. The center frequency f_c is 4.97 GHz. The lower cut-off f_L and upper cut-off f_H frequencies are 3.75 GHz and 6.6 GHz, respectively, and the bandwidth *BW* is 2.85 GHz.

In this design, the microstrip-based low-pass filter structure determines the lower cut-off frequency of the PCHM-SIW bandstop filter. In addition to this, the SIW-based high-pass filter structure determines the upper cut-off frequency of the PCHM-SIW bandstop filter [11], [12].

A. Step 1: The Design of the Conventional SIW-Based High-Pass Filter (S-HPF)

SIW structures were developed to transform rectangular volumetric waveguides into planar. As is known, SIW structures behave just like rectangular waveguides as high-pass filters and transmit in TE_{10} mode [12], [13].

The 2D layout geometry and simulated results of the SIW-based high-pass filter are given in Fig. 1(a). The Roger 4003C PCB substrate with good transmission values at high frequencies is preferred in the design (relative permittivity (ε_r) = 3.55, loss tangent (tan δ) = 0.0027, and substrate height (*h*) = 1.52 mm).

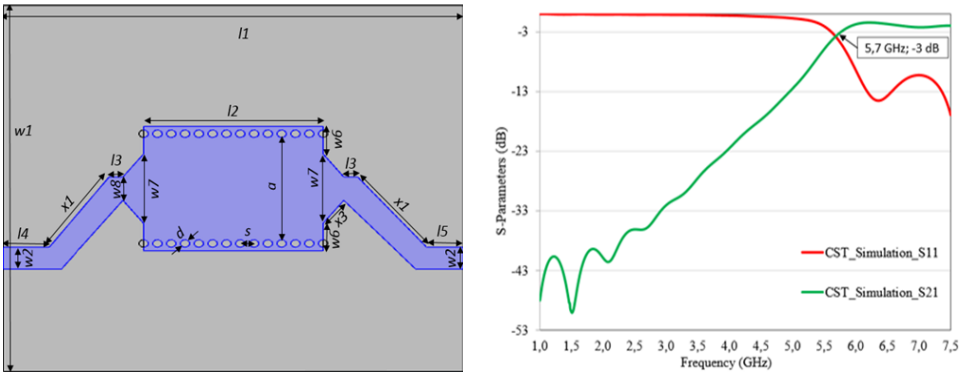

(a) (b)

Fig. 1. SIW-based high-pass filter: (a) 2D layout geometry (top view); (b) Simulated results.

The parameters along with their dimension values for the SIW-based high-pass filter are given in Table I.

TABLE I. SIW-BASED HIGH-PASS FILTER PARAMETERS AND DIMENSION VALUES.

Filter Parameter	Dimension (mm)	Filter Parameter	Dimension (mm)
a	17	l_5	4
s	1.50	w_1	40
h	1.52	w_2	3
d	1	w_6	3.75
l_1	50	w_7	9.50
l_2	19.50	w_8	3.20
l_3	1.50	x_1	12.18
l_4	5	x_3	3.15

A SIW or rectangular waveguide has a dominant TE mode. This dominant mode is TE_{10} (m = 1, n = 0). For this SIW-based high-pass filter, the cut-off wavelength ($\lambda_{c,\ hpf}$) is found by (1) and (2) as 28.61 mm. The cut-off frequency and wavelength of the substrate integrated waveguide [14]:

$$2\pi f_c = \omega_c = \frac{1}{\sqrt{\mu_0 \varepsilon}} \sqrt{\left(\frac{m\pi}{a}\right)^2 + \left(\frac{n\pi}{b}\right)^2}, \quad (1)$$

$$\lambda_{c_{hpf}} = \frac{c}{f_c \sqrt{\varepsilon_r}}, \quad (2)$$

where m and n are the values of the TE mode, a is the width of the filter, b is the height of the filter, c is the speed of light, f_c is the cut-off frequency, ε_r is the relative permittivity, ε is the permittivity of substrate, and μ_0 is the magnetic permeability of the free space.

As presented in Fig. 1(b), the frequency rejection is good in the CST Studio Suite simulation. S_{11} (return loss) appears to be larger than 10 dB in the passband (in-band). S_{21} (insertion loss) appears to be less than 1.5 dB in the passband (5.7 GHz–7.5 GHz). In the CST simulation, the cut-off frequency is acquired to be f_c = 5.7 GHz. From Fig. 1(b), the suppression at out-of-band is around 20 dB. The SIW filter transmits passband signals with good performance [15], [16].

B. Step 2: The Design of the Microstrip-Based Low-Pass Filter (M-LPF)

The procedure for designing a low-pass microstrip-based filter is to cascade λ/8 transmission lines that have remarkably high and low characteristic impedances (hi-Z, low-Z). Stepped impedance is used to design the low-pass microstrip-based filter in this study. A fifth-order Chebyshev microstrip low-pass filter with a ripple factor of 3 dB is realised on the

RO4003C substrate by the step impedance method for a cut-off frequency of 3.75 GHz [11], [17]. The Roger 4003C PCB substrate is preferred in filter designs due to its microwave frequency performance and reducing the circuit production cost. Due to the low dielectric loss property of the RO4003C PCB substrate, they can be used in most applications in which conventional materials present difficulties and higher losses at high frequencies.

In Fig. 2, the geometry (top view) of low-pass filter on a microstrip substrate with cut-off frequency of 3.75 GHz is given along with the corresponding variables in the design.

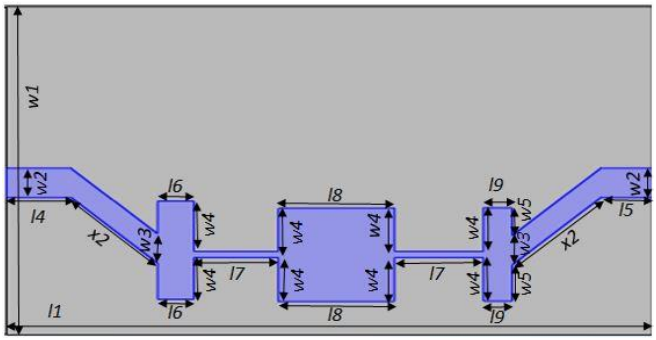

Fig. 2. Top view of the designed microstrip-based low-pass filter.

The parameters along with their dimension values of the designed low-pass filter on a microstrip are given in Table II.

TABLE II. THE MICROSTRIP-BASED LOW-PASS FILTER PARAMETERS AND DIMENSION VALUES.

Filter Parameter	Dimension (mm)	Filter Parameter	Dimension (mm)
x_2	9.69	l_1	50
w_1	40	l_4	5
w_2	3	l_6	2.78
w_3	3	l_7	6.56
w_4	4.40	l_8	8.99
w_5	3.24	l_9	2.23
l_1	50	h	1.52

The design of the fifth-order Chebyshev low-pass filter is based on the insertion loss method. Passive circuit elements of the fifth-order Chebyshev low-pass filter are calculated for the characteristic impedance (Z_0) of 50 Ω, and the filter order (N) of 5. The passive circuit elements and the low-pass filter values are found as $C_1 = C_5$ =2.955 pF, $L_2 = L_4$ = 1.617 nH, and C_3 = 3.852 pF. In Fig. 3(a), the equivalent electric circuit of the fifth-order Chebyshev low-pass filter is represented. The fifth-order Chebyshev microstrip low-pass filter has a calculated wavelength of λ_{lpf} = 43.37 mm for 3.75 GHz using (2). Furthermore, the S-parameters of the microstrip-based low-pass filter are obtained in the CST Studio Suite for the range of 6.5 GHz, and the simulation results are represented in Fig. 3 (b). As presented in Fig. 3(b), the band rejection of the simulation is close to the analysis. It can be observed that the transition band in the analysis is evaluated to be narrower than the transition band in the simulation.

On the other hand, the values of the S_{21} parameter in the band in the simulation are slightly worse than those of the analysis. The simulation results differ slightly from the analytical results due to the design of the broadband bandstop filter. In the CST simulation, the cut-off frequency is obtained as 2.91 GHz. The analysis value is also 3.75 GHz. The cut-off frequency change in the simulation according to the analytical value is 22.4 %.

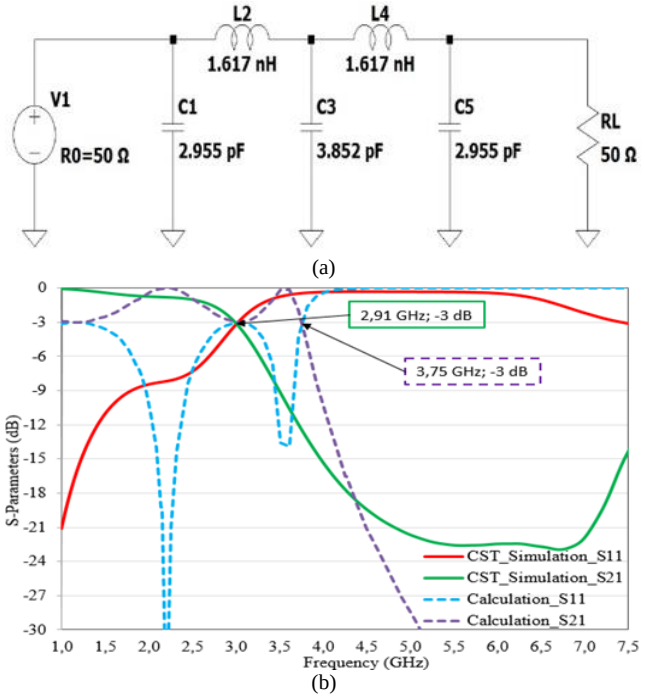

Fig. 3. The microstrip-based low-pass filter: (a) The equivalent circuit model of the fifth-order Chebyshev; (b) The calculated and simulated results.

C. Step 3: Design of Parallel Connected Hybrid Microstrip-SIW Bandstop Filter

In Table III, the parameters and all corresponding dimensions of the PCHM-SIW bandstop filter, are presented.

TABLE III. THE PCHM-SIW BANDSTOP FILTER PARAMETERS AND DIMENSION VALUES.

Filter Parameter	Dimension (mm)	Filter Parameter	Dimension (mm)
a	17	l_1	50
s	1.50	l_2	19.50
h	1.52	l_3	1.50
d	1	l_4	5
w_1	40	l_5	4
w_2	3	l_6	2.78
w_3	3	l_7	6.56
w_4	4.40	l_8	8.99
w_5	3.24	l_9	2.23
w_6	3.75	x_1	12.18
w_7	9.50	x_2	9.69
w_8	3.20	x_3	3.15

The 2D/3D geometry of the two-port PCHM-SIW bandstop filter and its parameters are given in Fig. 4. Also the connection angle between the transmission lines of two parallel connected structures is 120 degrees.

Equations (3)–(13) have been used in the design of the bandstop through an integrated microstrip-substrate waveguide [11], [18]. The center frequency of the PCHM-SIW bandstop filter is formulated as ω_0 in (3) such that

$$\omega_0 = \sqrt{\omega_1 \omega_2}. \quad (3)$$

The fractional bandwidth (FBW) of the PCHM-SIW bandstop filter is also expressed with (4) as

$$\Delta = \frac{\omega_2 - \omega_1}{\omega_0}. \quad (4)$$

A series inductor, L_k, is converted to a series liquid crystal (LC) circuit with element values:

$$L_k' = \frac{\mathrm{L_k}}{\Delta\omega_0}, \quad (5)$$

$$C_k' = \frac{\Delta}{\omega_0 \mathrm{L_k}}. \quad (6)$$

A shunt capacitor, C_k, is converted to a parallel LC circuit with element values:

$$L_k' = \frac{\Delta}{\omega_0 \mathrm{C_k}}, \quad (7)$$

$$C_k' = \frac{\mathrm{C_k}}{\Delta\omega_0}. \quad (8)$$

The transfer function, S_{21}, is usually written in decibels and is known in the literature as the insertion loss (L_A)

$$L_A = -20\log_{10}\left|S_{21}(j\omega)\right| dB. \quad (9)$$

The reflection coefficient of S_{11} expressed in decibels is called the return loss (L_R) of the filter

$$L_R = -20\log_{10}\left|S_{12}(j\omega)\right| dB. \quad (10)$$

The propagation constant is expressed as

$$\beta = \sqrt{\left(\omega^2\mu\varepsilon\right) - \left(\frac{\pi}{a}\right)^2}. \quad (11)$$

The guided wavelength, λ_g, is expressed in terms of β,

$$\lambda_g = \frac{2\pi}{\beta} = \frac{\lambda_0}{\sqrt{1-\left(\frac{\omega_c}{\omega}\right)^2}}. \quad (12)$$

The wave impedance of the TE mode, Z_{TE} is known as

$$Z_{TE} = \frac{\omega\mu}{\beta} = \frac{\omega\mu\lambda g}{2\pi} = \frac{\eta}{\sqrt{1-\left(\frac{\omega_c}{\omega}\right)^2}}. \quad (13)$$

The insertion loss method is used in the design of the PCHM-SIW bandstop filter, where the values of elements in the equivalent circuit of the PCHM-SIW bandstop filter are analysed for the characteristic impedance (Z_0) of 50 Ω and the filter order (N) of 5.

The passive circuit elements and values of the PCHM-SIW bandstop filter are C_1 = 1.276 pF, L_1 = 802.1 pH, C_2 = 1.466 pF, L_2 = 698.2 pH, C_3 = 1.663 pF, L_3 = 615.4 pH, C_4 = 1.466 pF, L_4 = 698.2 pH, C_5 = 1.276 pF, and L_5 = 802.1 pH.

The equivalent electric circuit of the bandstop filter with a ripple factor of 3 dB is shown in Fig. 5(a).

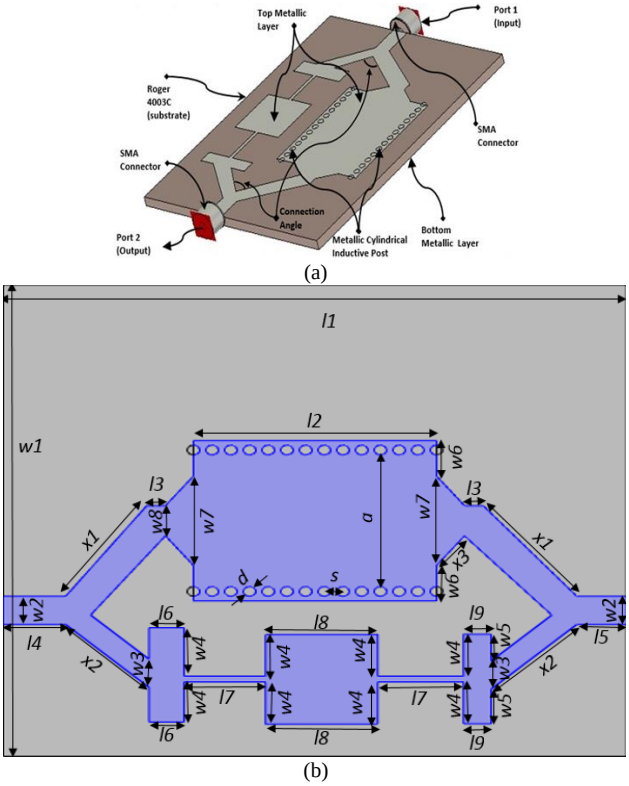

Fig. 4. The two-port PCHM-SIW bandstop filter: (a) 3D geometry (top view); (b) 2D layout geometry (top view) and parameters.

The wavelength (λ_{bsf}) of the PCHM-SIW bandstop filter is found to be 32.81 mm according to (1)–(3). The calculated bandwidth of stopband is 2.85 GHz. The simulated 3-dB BW is seen as 2.85 GHz in Fig. 5. Overall, the frequency rejection in the analysis is better than the simulation results. The center frequencies of simulation and analysis (f_c) are 4.26 GHz and 4.97 GHz, respectively.

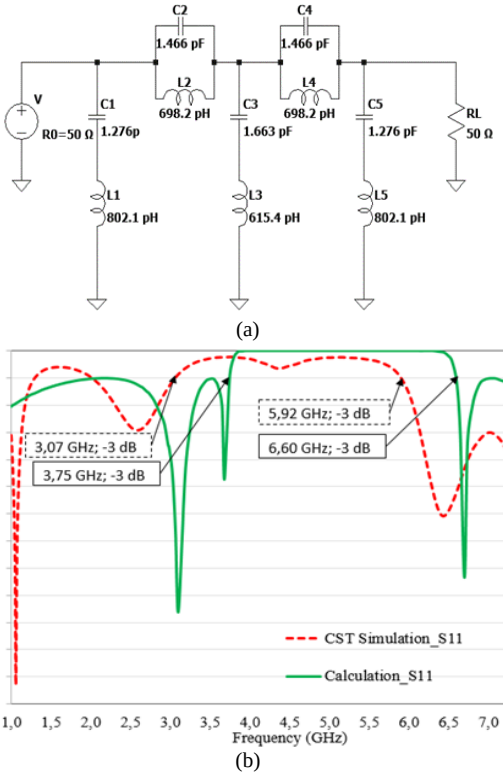

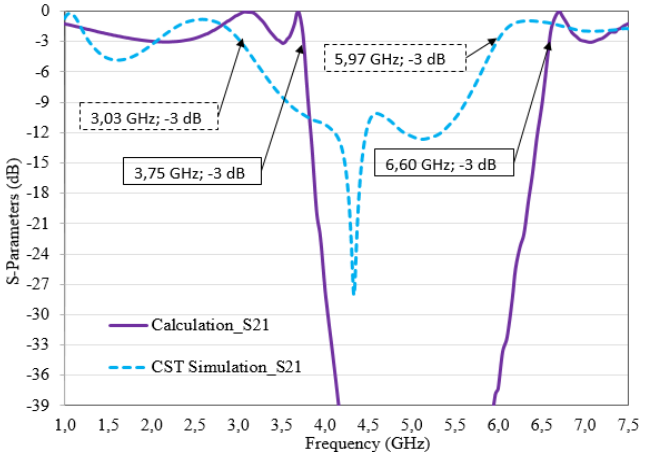

(c)

Fig. 5. PCHM-SIW bandstop filter: (a) Circuit equivalent of the fifth-order Chebyshev; (b) Calculation and CST simulation results (S_{11}); (c) Calculated and simulated results (S_{21}).

III. MANUFACTURE OF THE PCHM-SIW BANDSTOP FILTER AND EXPERIMENTAL RESULTS

Ceramic/hydrocarbon-based materials (RO4003C) are preferred due to their advanced microwave frequency performance and low-cost circuit manufacturing. This low-loss PCB material, which can be produced using standard processes, is used in microstrip-SIW filter design. This RO4003C PCB substrate is used for low-cost filter production with a PCB prototyping machine (MITS Autolab). The PCHM-SIW bandstop filter, which is manufactured using a Roger PCB substrate, is depicted in Fig. 6. The metallic connection/contact between the top and bottom (ground) sides of the PCB is achieved by soldering the pins with a diameter of 1 mm, which pass through the holes. The compact size of the manufactured PCHM-SIW bandstop filter is 50 mm × 40 mm × 1.52 mm.

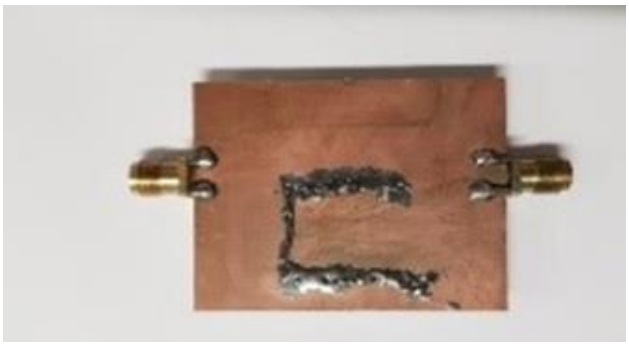

(a)

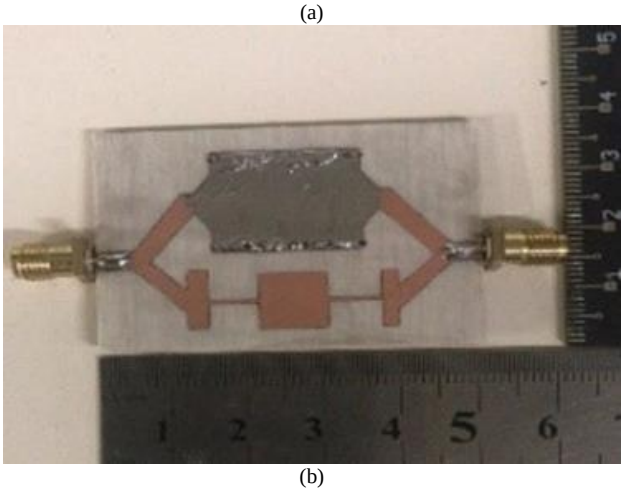

(b)

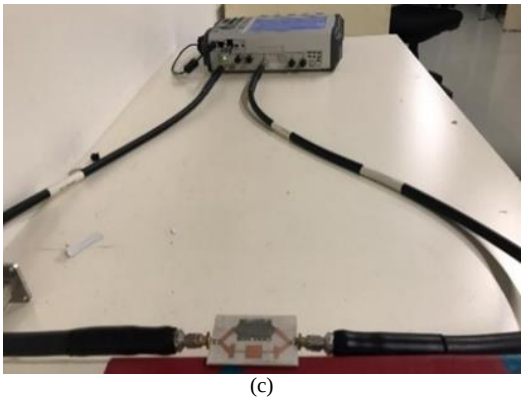

(c)

Fig. 6. The two-port PCHM-SIW bandstop filter fabricated: (a) View from the bottom; (b) View from the top; (c) Measurement with the network analyser.

The PCHM-SIW bandstop filter is produced at Yasar University Antenna and Microwave Laboratory. The manufactured filter is measured by a vector network analyser (Anritsu-VNA Master MS2028C). The frequency responses of the PCHM-SIW bandstop filter are tested at 1001 frequency points where the sampling frequency, f_s, is 6.5 kHz. The measurement and simulation frequency ranges 1 GHz to 7.5 GHz. The PCHM-SIW bandstop filter during measurement in the laboratory is depicted in Fig. 6(c).

It is shown in Fig. 7 that the 3-dB measurement bandwidth is 2.65 GHz ($|S_{11}| > -3$ dB). Furthermore, the lower and upper cut-off frequencies are measured as f_L = 2.98 GHz and f_H = 5.63 GHz, respectively. The center frequency of the measurement is f_c = 4.1 GHz. The L_R in the measurement is generally less than 1.98 dB in the stopband.

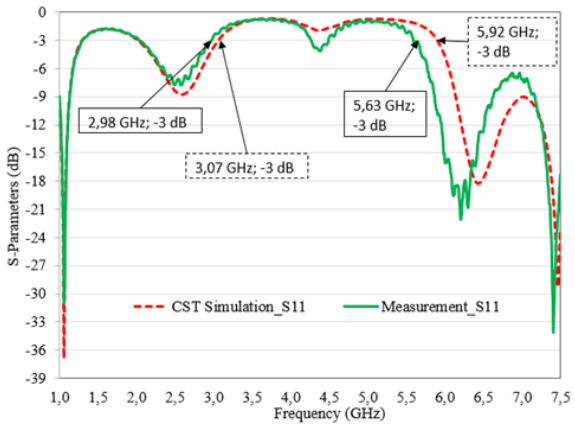

(a)

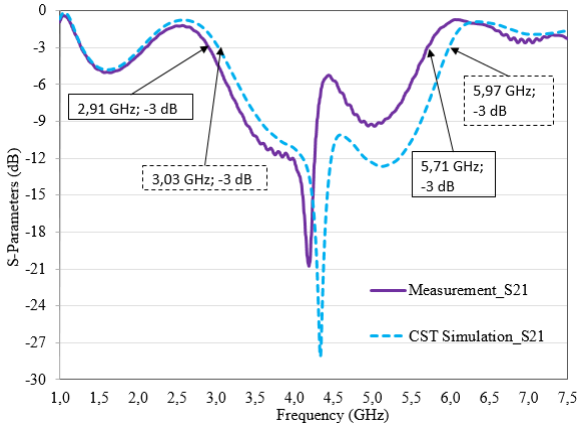

(b)

Fig. 7. CST simulation and measurement results for PCHM-SIW bandstop filter: (a) Return loss; (b) Insertion loss.

L_A is normally bigger than 9 dB in the stopband. It is seen that there is a ripple between 4.4 GHz and 4.6 GHz in the S_{11} and S_{21} parameters. This is thought to be due to the transition between low- and high-pass filter cut-off frequencies. In Table IV, the calculated, simulation, and measured results are given together.

TABLE IV. CALCULATION, SIMULATION, AND MEASUREMENT RESULTS OF PCHM-SIW BANDSTOP FILTER.

Operation	Lower -3 dB Cut-off Freq. (f_L) (GHz)	Center Freq. (f_c) (GHz)	Upper -3 dB Cut-off Freq. (f_H) (GHz)	Bandwidth (BW) (GHz)
Calculation	3.75	4.97	6.60	2.85
Simulation	3.07	4.26	5.92	2.85
Measurement	2.98	4.10	5.63	2.65

The simulation and measurement results of the broadband bandstop filter designed for the 1 GHz to 7.5 GHz operating region deviated slightly from the analytical results. This is thought to be due to difficulties in designing and implementing the bandstop filter as a broadband filter covering the C-Band and S-Band. It is thought that additional losses occur in filter production.

A comparison of the recent published SIW bandstop filters is given in Table V. According to Table V, the highest transmission loss value exists in the study of the authors in [19], the lowest return loss value is in the study of the authors in [20], and the highest *FBW* value is in this work.

TABLE V. THE COMPARISON OF RESULTS OF DIFFERENT SIW BANDSTOP FILTERS.

Ref.	Type of Design	Type of Filter	Center Freq. (GHz) *FBW* (%)	ε_r tanδ	RL (dB)	IL (dB)
[6]	Coaxial Resonator-SIW	Bandstop	3.73 12.5 %	3.32 0.002	<2 dB	>20 dB
[19]	Via-hole resonator-SIW	Bandstop	10.74 14.7 %	2.94 0.0012	≤1.8 dB	≥32 dB
[20]	Radial Resonator-SIW	Bandstop	9.26 5.47 %	3.48 0.0037	≤1.3 dB	≥18 dB
[21]	Split-Ring Resonator-SIW	Bandstop	3.5 11.4 %	10.2 0.0023	≤1.9 dB	≥25 dB
This work	Microstrip-SIW	Bandstop	4.26 66.9 %	3.38 0.0027	<1.98 dB	≥9 dB

*Note: *ε_r, FBW, tanδ, RL, and IL correspond to dielectric constant, fractional bandwidth, loss tangent, return loss, and insertion loss, respectively.*

The bandstop frequency band of the proposed filter structure is between almost 3 GHz and 5.65 GHz. One suitable application of this filter can be about second- and/or third-harmonic suppressions of several wireless communication systems. For instance, applications within frequency band between 1.5 GHz and 2.8 GHz such as GPS L1, ISM/Wi-Fi 2.4 GHz, GSM 1800, 3G/4G have carrier signals whose second harmonics fall into the stopband region of the proposed filter. Similarly, the third harmonics of the communication systems, whose operating frequency bands are placed within 1 GHz to about 1.9 GHz, such as all GPS, GNSS, Glonass bands, GSM 1800, etc., are again kept inside the stopband of the filter.

IV. CONCLUSIONS

In this study, the parallel connection model of separate filter structures is discussed. It is shown that the low-pass filter and the high-pass filter, whose frequency response behaviours are shown separately, create a bandstop filter effect when combined with parallel connection. The development of such modular hybrid filter structures is much easier than that for compact filter structures.

The SIW-based high-pass filter effect can be clearly observed in the frequency response of the bandstop filter. On the contrary, the microstrip-based low-pass filter S_{11} parameters deviate slightly from the expected frequency response. The low-pass filter design is based on its λ/8. The simulated S_{21} is greater and equal to about 10 dB, whereas the simulated S_{11} is less than 3 dB. The measured S_{11} and S_{21} are generally consistent with the simulation results except for several frequency regions. The bandwidth values acquired from simulation and measurement for the PCHM-SIW bandstop filter are 2.85 GHz and 2.65 GHz, respectively. This filter structure can be considered as a good candidate for S- and C-bands on which undesired signals can be effectively suppressed to eliminate any interference or noise effects.

CONFLICTS OF INTEREST

The authors declare that they have no conflicts of interest.

REFERENCES

[1] R. J. Cameron, C. M. Kudsia, and R. R. Mansour, *Microwave Filters for Communication Systems*, 2nd ed., John Wiley & Sons, Inc., NJ, 2018. DOI: 10.1002/9781119292371.

[2] D. Deslandes and K. Wu, "Integrated microstrip and rectangular waveguide in planar form", *IEEE Microw. & Wireless Components Lett.*, vol. 11, no. 2, pp. 68–70, 2001. DOI: 10.1109/7260.914305.

[3] S. Awasthi, A. Biswas, and M. J. Akhtar, "Dual-band dielectric resonator bandstop filters", *Int. Journal of RF and Microw. Computer-Aided Eng.*, vol. 25, no. 4, pp. 282–288, 2014. DOI: 10.1002/mmce.20860.

[4] W. Xu *et al.*, "Tunable bandstop HMSIW filter with flexible center frequency and bandwidth using liquid crystal", *IEEE Access*, vol. 7, pp. 161308–161317, 2019. DOI: 10.1109/ACCESS.2019.2951543.

[5] E. A. Casu *et al.*, "Vanadium oxide bandstop tunable filter for Ka frequency bands based on a novel reconfigurable spiral shape defected ground plane CPW", *IEEE Access*, vol. 6, pp. 12206–12212, 2018. DOI: 10.1109/ACCESS.2018.2795463.

[6] D. Psychogiou and R. Gómez-García, "Compact substrate-integrated bandstop filters using double-resonant coaxial resonators", *IEEE Microw. and Wireless Components Lett.*, vol. 30, no. 10, pp. 941–944, 2020. DOI: 10.1109/LMWC.2020.3019232.

[7] G. Zheng and J. Papapolymerou, "Monolithic reconfigurable bandstop filter using RF MEMS switches", *Int. Journal of RF and Microw. Computer-Aided Eng.*, vol. 14, no. 4, pp. 373–382, 2004. DOI: 10.1002/mmce.20018.

[8] A. Gorur and C. Karpuz, "Reduced-size wideband bandstop filter using two open-circuited shunt stubs spaced by a double-length transmission-line element", *Int. Journal of RF and Microw. Computer-Aided Eng.*, vol. 15, no. 1, pp. 79–85, 2005. DOI: 10.1002/mmce.20053.

[9] F. F. He, K. Wu, and W. Hong, "A wideband bandpass filter by integrating a section of high pass HMSIW with a microstrip lowpass filter", in *Proc. of 2008 Global Symposium on Millimeter Waves*, 2008, pp. 282–284. DOI: 10.1109/GSMM.2008.4534623.

[10] V. Nova *et al.*, "Thermal stability analysis of filters in substrate integrated technologies under atmospheric pressure and vacuum conditions", *IEEE Access*, vol. 8, pp. 118072–118082, 2020. DOI: 10.1109/ACCESS.2020.3004875.

[11] A. Jubril and S. D. Nyitamen, "2 GHz microstrip low pass filter design with open-circuited stub", *IOSR Journal of Electr. and Comm. Eng. (IOSR-JECE)*, vol. 13, no. 2, pp. 01–09, 2018. DOI: 10.9790/2834-1302020109.

[12] H. Y. Xie, B. Wu, L. Xia, J. Z. Chen, and T. Su, "Miniaturized half-mode fan-shaped SIW filter with extensible order and wide stopband",

IEEE Microw. and Wireless Components Lett., vol. 30, no. 8, pp. 749–752. 2020. DOI: 10.1109/LMWC.2020.3001092.

[13] K. Guvenli, S. Yenikaya, M. Secmen, and C. Turkmen, "The modular design of M-SIW wideband band-stop filter", in *Proc. of 2020 IEEE Ukrainian Microwave Week*, 2020, pp. 1079–1082. DOI: 10.1109/UkrMW49653.2020.9252676.

[14] L.-F. Qiu, L.-S. Wu, W.-Y. Yin, and J.-F Mao, "Hybrid non-uniform-*Q* lossy filters with substrate integrated waveguide and microstrip resonators", *IET Microw., Antennas & Propag.*, vol. 12, no. 1, pp. 92–98, 2018. DOI: 10.1049/iet-map.2017.0060.

[15] K. Guvenli, S. Yenikaya, and M. Secmen, "Analysis, design, and actual fabrication of a hybrid microstrip-SIW bandpass filter based on cascaded hardware integration at X-band", *Elektronika ir Elektrotechnika*, vol. 27, no. 1, pp. 23–28, 2021. DOI: 10.5755/j02.eie.27479.

[16] A. O. Nwajana, A. Dainkeh, and K. S. K. Yeo, "Substrate integrated waveguide (SIW) bandpass filter with novel microstrip-CPW-SIW input coupling", *Journal of Microw., Optoelectronics and Electromagnetic Appl.*, vol. 16, no. 2, pp. 393–402, 2017. DOI: 10.1590/2179-10742017v16i2793.

[17] S. Mitra and D. K. Kumuda, "Stepped impedance microstrip low-pass filter implementation for S-band application", *Int. Journal of Latest Trends in Engineering and Techn.*, vol. 5 no. 3, pp. 248–255, 2015.

[18] I. Hunter, *Theory and Design of Microwave Filters*. London: The Institution of Engineering and Technology, 2001.

[19] M. Esmaeili, J. Bornemann, and P. Krauss, "Substrate integrated waveguide bandstop filter using partial-height via-hole resonators in thick substrate", *IET Microw., Antennas & Propag.*, vol. 9, no. 12, pp. 1307–1312, 2015. DOI: 10.1049/iet-map.2015.0141.

[20] M. N. Husain, G. S. Tan, and K. S. Tan, "Enhanced performance of substrate integrated waveguide bandstop filter using circular and radial cavity resonator", *Int. Journal of Engineering and Tech.*, vol. 6, no. 2, pp. 1268–1277, 2014.

[21] J. Hinojosa, M. Rossi, A. Saura-Ródenas, A. Álvarez-Melcón, and F. L. Martínez-Viviente, "Compact bandstop half-mode substrate integrated waveguide filter based on a broadside-coupled open split-ring resonator", *IEEE Trans. on Microw. Theory and Techn.*, vol. 66, no. 6, pp. 3001–3010, 2018. DOI: 10.1109/TMTT.2018.2833483.